Central European Journal of Energetic Materials, **2012**, *9*(1), 59-76
ISSN 1733-7178

Charge Density Distribution, Electrostatic Properties and Sensitivity of the Highly Energetic Molecule 2,4,6-Trinitro-1,3,5-triazine: A Theoretical Study

P. SRINIVASAN, K. MAHESHWARI, M. JOTHI
and P. KUMARADHAS*

Department of Physics, Periyar University,
Salem − 636 011, India
**E-mail: kumaradhas@yahoo.com*

Abstract: *Ab initio* and density functional theory (DFT) calculations were carried out on the energetic propellant molecule 2,4,6-trinitro-1,3,5-triazine (TNTA) to understand its bond topology and its energetic properties using the theory of atoms in molecules (AIM). The DFT method predicts that the electron density $\rho_{bcp}(r)$ at the bond critical points of ring C–N bonds is ~2.34 eÅ^{-3} and the corresponding Laplacian $\nabla^2\rho_{bcp}(r)$ is ~ -24.4 eÅ^{-5}; whereas these values are found to be very small in the $-NO_2$ group attached to C–N bonds [$\rho_{bcp}(r)$: ~1.73 eÅ^{-3} and $\nabla^2\rho_{bcp}(r)$: ~ -14.5 eÅ^{-5}]. The negative Laplacian values of C–NO_2 bonds are significantly lower which indicates that the charges of these bonds are highly depleted. The C–NO_2 bonds exhibit low bond order (~0.8), as well as low (~56.4 kcal/mol) bond dissociation energy. As we reported in our earlier studies, we found high bond charge depletion for these bonds, which are considered the weakest bonds in the molecule. The frontier orbital energies exhibit a wide band gap, which is larger than those of existing molecules TATB, TNT and TNB. The impact sensitivity (H_{50}%) (4.2 m) and oxygen balance (2.77%) were calculated and compared with related structures. Large negative electrostatic potential regions were found near the nitro groups where reaction is expected to occur. The relation between charge depletion $\nabla^2\rho_{bcp}(r)$ and the electrostatic potential at the bond midpoints V_{mid} reveals the sensitive areas of the molecule.

Keywords: energetic molecule, electron density, Laplacian of electron density, electrostatic potential, impact sensitivity

Introduction

The process of synthesizing energetic materials and qualifying them for military use is not straightforward. It can be tedious, expensive and hazardous. Wasteful empirical testing of energetic materials may be replaced by computer simulations prior to experimental exploration. In recent decades, significant effort has been made to design new energetic materials with low signature and low shock sensitivity and a large number of nitro derivatives has been studied [1-6]. Furthermore, it has been reported that there are some correlations between charge separation in the molecules (as measured by the charge density distribution, Laplacian of electron density and surface electrostatic potential) and the impact sensitivity [7, 8]. Thus, the pattern of charge distribution and ESP are core ways for deciding the impact sensitivity of explosives. We have extended our study to the investigation of high energy molecules, such as new potential rocket propellants and explosives. Recently, we have studied the charge density distribution, bond topology, electrostatic properties and the energy density distribution of a series of highly energetic molecules [7, 8]. As a continuation, we report here the charge density analysis of the molecule 2,4,6-trinitro-1,3,5-triazine (TNTA) (Figure 1). A recent theoretical study of this molecule reports that it is a potential propellant ingredient which exhibits a high heat of formation and specific impulse (I_{sp}), and zero oxygen balance; its performance is also very similar to RDX [9]. In 1977, Immirzi et al. estimated theoretically (volume additivity method) its density (~2.1 g/cm^3) which is significantly higher than RDX (~1.82 g/cm^3) [10, 11]. However, as far as we know, there is no experimental report on this molecule. The predicted energetic parameters indicate that TNTA is a potential energetic molecule; hence, it is worth further analysis.

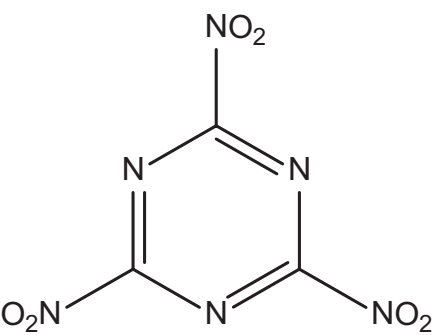

Figure 1. Chemical structure of 2,4,6-trinitro-1,3,5-triazine (TNTA).

Electron density $\rho_{bcp}(r)$ is an important parameter, useful for bond topological characterization which allows one to understand the reactivity and stability of molecular systems. The topological properties of the electron density $\rho(r)$ can be explored by the complete specification of its bond critical point (bcp) at which $\nabla\rho(r) = 0$. A critical point r_{bcp} is classified according to its rank and signature, which is designated as (λ, σ) [12]. The rank λ of a critical point is equal to the number of non-zero eigenvalues of the Hessien matrix of $\rho_{bcp}(r)$, whilst the signature σ is the algebraic sum of the signs of the eignvalues. Among the four non-degenerate critical points: (3,-3) (nucleus critical point), (3,+3) (cage critical point), (3,+1) (ring critical point), and (3,-1) (bond critical point), only the bond critical point is considered for this study [13]. The Laplacian of electron density is:

$$\nabla^2\rho = \frac{\partial^2\rho}{\partial x^2} + \frac{\partial^2\rho}{\partial y^2} + \frac{\partial^2\rho}{\partial z^2} \quad (1)$$

which identifies the region of space where the electron density is locally concentrated or depleted. The maximum negative value of $\nabla^2\rho_{bcp}(r)$ indicates that the electron density is locally concentrated if $\nabla^2\rho_{bcp}(r) < 0$ and depleted if $\nabla^2\rho_{bcp}(r) > 0$. The electron density may be correlated with local energy density H(r) in the bonding region [12], which is given as:

$$H(r) = G(r) + V(r) \quad (2)$$

where G(r) and V(r) are the local kinetic and potential energy density. V(r) is always negative and G(r) positive; the sign of H(r) indicates the dominant one in the bonding regions.

Computational details

The TNTA molecule has been optimized from the MP2 and BP86 levels with the basis set 6-311G*; these optimizations were converged at 0.000050, 0.000114 au respectively for the maximum force and 0.000018, 0.000051 au respectively for the root mean square (RMS) force. All these calculations were carried out using the GAUSSIAN03 program [14]. The wave function obtained from the optimization has been used for the charge density analysis. To understand the bond strength of the molecule, the bond topological parameters were calculated using the AIMPAC program [15]. Furthermore, the bond order [16] (on the basis of Wiberg's bond index) and the local energy density distribution of the molecule were also calculated. The deformation density and the Laplacian maps were plotted using *wfn2plots* and XD [17] software packages. The deformation

density of the molecule is defined as $\Delta\rho(r) = \rho_{mol}(r) - \rho_{ref}(r)$, where $\rho_{mol}(r)$ is the electron density of the molecule and $\rho_{ref}(r)$ is the reference density of the molecule [18]. The reference density distribution is the density of the neutral spherical ground state atom at each nuclear position of the bond [19]. The isosurface of electrostatic potential has been plotted using 3Dplot (WinXPRO) software [20] to identify the strong electropositive and negative regions of the molecule.

Results and Discussion

Structural aspects

The optimized structure of TNTA calculated at the MP2/6-311G* level is depicted in Figure 2 and the geometric values are presented in Table 1. The C–N bond distances of the aromatic ring optimized at MP2 and BP86 levels are ~1.301 and ~1.332 Å respectively and these values are found to be lower than those for a similar reported experimental structure (~1.352 Å) [21]. The C–NO_2 bond distances predicted by both methods i.e. ~1.474 (MP2) and ~1.507 Å (BP86), are unequal. These distances are much longer than the ring C–N bonds (1.301/1.332 Å) of the molecule. The N=O bond distance calculated from the MP2 level is ~1.178 Å, which is found to be lower than the distance predicted by the BP86 method (~1.226 Å), and these values are close to that reported for the TATB molecule (1.236 Å) [22].

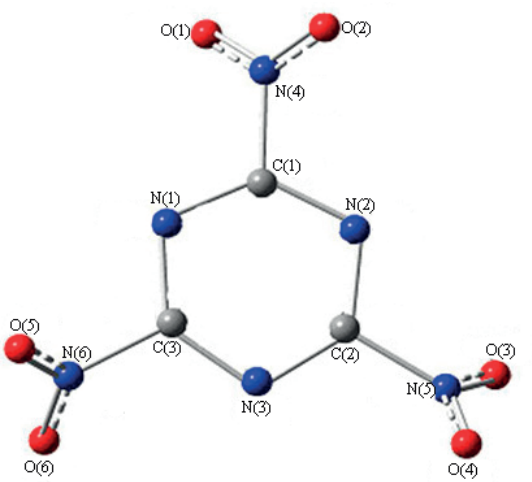

Figure 2. Optimized structure of the 2,4,6-trinitro-1,3,5-triazine molecule at the MP2/6-311G* level.

Table 1. Geometric parameters of the TNTA molecule

	MP2	BP86
Bond length (Å)		
C(1)–N(1)	1.301	1.332
C(3)–N(1)	1.301	1.332
C(1)–N(2)	1.301	1.332
C(1)–N(4)	1.474	1.507
C(2)–N(2)	1.301	1.332
C(2)–N(3)	1.301	1.332
C(2)–N(5)	1.474	1.507
C(3)–N(3)	1.301	1.332
C(3)–N(6)	1.474	1.507
N(4)–O(1)	1.178	1.226
N(4)–O(2)	1.178	1.226
N(6)–O(5)	1.178	1.226
N(6)–O(6)	1.178	1.226
N(5)–O(3)	1.178	1.226
N(5)–O(4)	1.178	1.226

	MP2	BP86
Bond angle (°)		
C(1)–N(1)–C(3)	112.4	111.6
N(1)–C(1)–N(2)	127.6	128.4
N(1)–C(1)–N(4)	116.2	115.8
N(2)–C(1)–N(4)	116.2	115.8
C(1)–N(2)–C(2)	112.4	111.6
N(2)–C(2)–N(3)	127.6	128.4
N(2)–C(2)–N(5)	116.2	115.8
N(3)–C(2)–N(5)	116.2	115.8
C(2)–N(3)–C(3)	112.4	111.6
N(1)–C(3)–N(3)	127.6	128.4
N(1)–C(3)–N(6)	116.2	115.8
N(3)–C(3)–N(6)	116.2	115.8
C(3)–N(6)–O(5)	115.7	115.6
C(3)–N(6)–O(6)	115.7	115.6
O(5)–N(6)–O(6)	128.7	128.9
C(2)–N(5)–O(3)	115.7	115.6
C(2)–N(5)–O(4)	115.7	115.6
O(3)–N(5)–O(4)	128.7	128.9
C(1)–N(4)–O(1)	115.7	115.6
C(1)–N(4)–O(2)	115.7	115.6
O(1)–N(4)–O(2)	128.7	128.9

	MP2	BP86
Torsion angle (°)		
C(3)–N(1)–C(1)–N(2)	0	0
C(3)–N(1)–C(1)–N(4)	180	179.9
C(1)–N(1)–C(3)–N(3)	0	0
C(1)–N(1)–C(3)–N(6)	180	180
N(1)–C(1)–N(2)–C(2)	0	-0.1
N(4)–C(1)–N(2)–C(2)	180	-180
N(1)–C(1)–N(4)–O(1)	128.9	123.8
N(1)–C(1)–N(4)–O(2)	-51.1	-56.3
N(2)–C(1)–N(4)–O(1)	-51.1	-56.3
N(2)–C(1)–N(4)–O(2)	128.9	123.7
C(1)–N(2)–C(2)–N(3)	0	0.1
C(1)–N(2)–C(2)–N(5)	180	180

	MP2	BP86
Torsion angle (°)		
N(5)–C(2)–N(3)–C(3)	-180	-179.9
N(2)–C(2)–N(5)–O(3)	128.8	124.2
N(2)–C(2)–N(5)–O(4)	-51.2	-55.9
N(3)–C(2)–N(5)–O(3)	-51.2	-55.9
N(3)–C(2)–N(5)–O(4)	128.8	124
C(2)–N(3)–C(3)–N(1)	0	0
C(2)–N(3)–C(3)–N(6)	-180	-180
N(1)–C(3)–N(6)–O(5)	-51.2	-56.1
N(1)–C(3)–N(6)–O(6)	128.8	123.9
N(3)–C(3)–N(6)–O(5)	128.8	123.9
N(3)–C(3)–N(6)–O(6)	-51.2	-56.1

All of the bond distances calculated from the BP86 level are significantly longer than those predicted from the MP2 level; these differences may be attributed to the methodological effects of energy minimization of the molecule. Since, the atoms N(1), N(3) and N(5) are in similar environments, the C(1)–N(2)–C(2) [111.6°], C(2)–N(3)–C(3) [111.6°] and C(3)–N(1)–C(1) [111.6°] bond angles are almost equal and the average value is ~111.6° (Table 1). Similar trends appears around the C(1), C(2) and C(3) atoms, the corresponding angle being ~127°. Furthermore, the O–N–O bond angles predicted by the MP2 and BP86 levels are also found to be almost equal [~128.7°]. The mean plane calculation of the aromatic ring confirms that the ring is planar, the nitro groups at the 2, 4 and 6 positions in the ring are inclined to the mean plane of the ring at an angle of about 45°.

Charge density

Figure 3(a-b) shows the deformation density of the TNTA molecule calculated at the MP2/6-311G* level. The complete spectrum of electron density distribution of the molecule obtained from the bond topological analysis is presented in Table 2. Both the MP2 and BP86 methods predict equal electron density at the bcp for all C–N bonds of the aromatic ring, the value being ~2.35 eÅ^{-3}. Whereas the electron density of –NO_2 groups attached to C–N bonds exhibit a substantially lower density [~1.73 (DFT) and ~1.83 eÅ^{-3} (MP2)] than the C–N bonds of the ring, these values are very close to those reported for the TATB molecule (~1.85 eÅ^{-3}) [22]. The low bond density of the C–N bonds is attributed to the delocalization caused by the nitro groups. The N=O bond density is ~3.33 eÅ^{-3}, which is the highest density in the molecule. A similar trend was already found in an experimentally reported molecule [21]. The large values of Wiberg's bond [16] orders [~1.39 (MP2) and ~1.53 (BP86)] for the N=O bonds confirm the double bond nature. The bond charge polarization of each bond was calculated (Table 2); specifically, the polarization of C–N bonds of the aromatic ring [~12.9% (MP2) and ~11.0% (DFT)] was found to be much higher than the nitro group attached to C–N bonds [~8.3(MP2) and ~6.7%(DFT)].

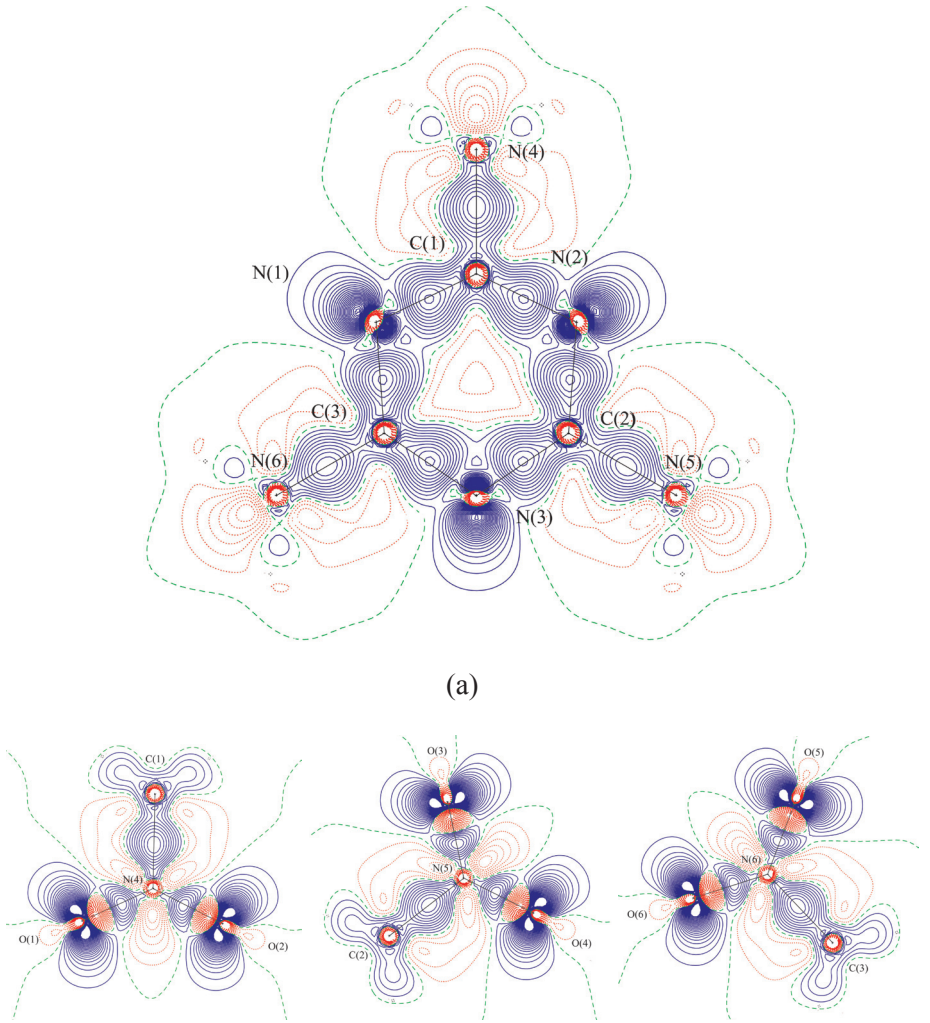

Figure 3. Deformation of electron density in the TNTA molecule (a) in the molecular plane and (b) in the NO_2 fragments. The positive contours (solid lines) and negative contours (dotted lines) are drawn at 0.05 eÅ^{-3} intervals. The zero contours are dashed lines.

Table 2. Bond topological properties of the TNTA molecule (first line for BP86 and second line for MP2).

Bonds	$\rho_{bcp}(r)^a$	$\nabla^2\rho_{bcp}(r)^b$	ε	$\lambda_1{}^b$	$\lambda_2{}^b$	$\lambda_3{}^b$	$d_1{}^c$	$d_2{}^c$	D	Δd%	$G(r)^d$	$V(r)^d$	$H(r)^d$
C(1)–N(1)	2.34	-24.5	0.13	-17.9	-15.8	9.1	0.52	0.81	1.33	11	1.41	-4.65	-3.24
	2.35	-24.4	0.15	-18.1	-15.6	9.3	0.49	0.84	1.33	13	1.79	-5.29	-3.50
C(3)–N(1)	2.34	-24.5	0.13	-17.9	-15.8	9.1	0.52	0.81	1.33	11	1.41	-4.65	-3.24
	2.35	-24.4	0.15	-18.1	-15.6	9.3	0.49	0.84	1.33	13	1.79	-5.29	-3.50
C(3)–N(3)	2.34	-24.5	0.13	-17.9	-15.8	9.1	0.52	0.81	1.33	11	1.41	-4.65	-3.24
	2.35	-24.4	0.15	-18.1	-15.6	9.3	0.49	0.84	1.33	13	1.79	-5.29	-3.50
C(2)–N(3)	2.34	-24.5	0.13	-17.9	-15.8	9.1	0.52	0.81	1.33	11	1.41	-4.65	-3.24
	2.35	-24.4	0.15	-18.1	-15.6	9.3	0.49	0.84	1.33	13	1.79	-5.29	-3.50
C(2)–N(2)	2.34	-24.5	0.13	-17.9	-15.8	9.1	0.52	0.81	1.33	11	1.41	-4.65	-3.24
	2.35	-24.4	0.15	-18.1	-15.5	9.3	0.49	0.84	1.33	13	1.79	-5.29	-3.50
C(1)–N(2)	2.34	-24.5	0.13	-17.9	-15.8	9.1	0.52	0.81	1.33	11	1.41	-4.65	-3.24
	2.35	-24.4	0.15	-18.1	-15.6	9.3	0.49	0.84	1.33	13	1.79	-5.29	-3.50
C(1)–N(4)	1.73	-14.5	0.10	-13.4	-12.5	11.3	0.65	0.86	1.51	6.7	0.57	-2.2	-1.63
	1.83	-18.3	0.10	-14.5	-13.2	9.5	0.62	0.86	1.48	8.3	0.68	-2.64	-1.96
N(4)–O(1)	3.33	-22.7	0.10	-30.7	-27.8	35.8	0.58	0.65	1.23	2.6	2.49	-6.78	-4.29
	3.32	-23.6	0.12	-30.5	-27.2	34.1	0.55	0.65	1.23	4.1	2.75	-7.16	-4.40
N(4)–O(2)	3.33	-22.7	0.10	-30.7	-27.8	35.8	0.58	0.65	1.23	2.6	2.49	-6.78	-4.29
	3.32	-23.6	0.12	-30.5	-27.2	34.1	0.55	0.65	1.23	4.1	2.75	-7.16	-4.40
C(2)–N(5)	1.73	-14.5	0.10	-13.4	-12.5	11.3	0.65	0.86	1.51	6.7	0.57	-2.2	-1.63
	1.83	-18.3	0.10	-14.5	-13.2	9.5	0.62	0.86	1.48	8.3	0.68	-2.64	-1.96
N(5)–O(4)	3.33	-22.7	0.10	-30.7	-27.8	35.8	0.58	0.65	1.23	2.6	2.49	-6.78	-4.29
	3.32	-23.6	0.12	-30.5	-27.2	34.1	0.55	0.65	1.23	4.1	2.75	-7.16	-4.40
N(5)–O(3)	3.33	-22.7	0.10	-30.7	-27.8	35.8	0.58	0.65	1.23	2.6	2.49	-6.78	-4.29
	3.32	-23.6	0.12	-30.5	-27.2	34.1	0.55	0.65	1.23	4.1	2.75	-7.16	-4.40
C(3)–N(6)	1.73	-14.5	0.10	-13.4	-12.5	11.3	0.65	0.86	1.51	6.7	0.57	-2.2	-1.63
	1.83	-18.3	0.10	-14.5	-13.2	9.5	0.62	0.86	1.48	8.3	0.68	-2.64	-1.96
N(6)–O(5)	3.33	-22.7	0.10	-30.7	-27.8	35.8	0.58	0.65	1.23	2.6	2.49	-6.78	-4.29
	3.32	-23.6	0.12	-30.5	-27.2	34.1	0.55	0.65	1.23	4.1	2.75	-7.16	-4.40
N(6)–O(6)	3.33	-22.7	0.10	-30.7	-27.8	35.8	0.58	0.65	1.23	2.6	2.49	-6.78	-4.29
	3.32	-23.6	0.12	-30.5	-27.2	34.1	0.55	0.65	1.23	4.1	2.75	-7.16	-4.40

[a] The electron density $\rho_{bcp}(r)$ ($eÅ^{-3}$), [b] Laplacian of electron density $\nabla^2\rho_{bcp}(r)$ ($eÅ^{-5}$), [c] d_1 and d_2 are the distances in Å between CP and the respective atoms of the bond, [d] Energy density ($HÅ^{-3}$).

Laplacian of charge density and energy density

The Laplacian of charge density $\nabla^2\rho_{bcp}(r)$ at the bcp provides significant information about the charge concentration and depletion in chemical bonds. Figure 4 shows the negative Laplacian of electron density of the molecule drawn in the molecular plane and the three $–NO_2$ fragments. To classify the bonds in the molecule, information concerning the existence of a negative Laplacian

and the local energy density H(r) of the bonds is required. The Laplacian of electron density and the energy density for all of the bonds were calculated. Both methods predict a high negative Laplacian for C_{ar}–N_{ar} (~ -24.4 eÅ^{-5}) and N=O bonds (~ -23.6 eÅ^{-5}), which indicates that the charges of these bonds are highly concentrated, and this matches well with the theoretically reported molecule [22]. This is further confirmed from the energy density distribution where these bonds exhibit high potential energy density V(r) [C_{ar}–$N_{ar:}$ ~ -5.29 (MP2); ~ -4.65 (BP86) and N=O: ~ -7.15 (MP2); ~ -6.78 HÅ^{-3} (BP86)]. The MP2 and DFT methods predict a low negative $\nabla^2\rho_{bcp}(r)$ value for the C–NO_2 bonds i.e. ~ -18.2 and ~ -14.5 eÅ^{-5}, respectively. The low negative value of the Laplacian indicates that the charges of these bonds are highly depleted. Both levels of theory predict almost the same bond order for the C–NO_2 bonds (value ~0.8), which is estimated by Wiberg's bond index [25]. The potential energy density V(r) of C–NO_2 bonds is ~ -2.6(MP2)/-2.2(BP86) and their total energy density H(r) is ~ -1.96 (MP2)/-1.63 (BP86). From the above bond topological parameters, it is confirmed that the C–NO_2 bonds are the weakest bonds in the molecule.

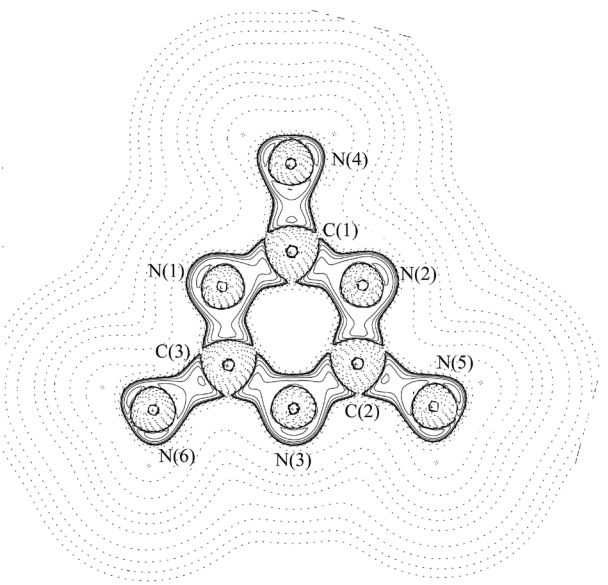

Figure 4. The Laplacian of electron density of the TNTA molecule. Contours are drawn at logarithmic intervals, 3.0 X 2^N eÅ^{-5}, where N = 2,4 and 8×10n, n = -2,-1,0,1,2 . Solid lines are positive contours; dashed lines are negative contours.

The bond ellipticity [23] is the measure of anisotropy of electron density distribution at the bcp of bonds. It can be calculated from the ratio of negative eigenvalues i.e. $\varepsilon = (\lambda_1/\lambda_2) - 1$, where λ_1 and λ_2 are the negative eigenvalues of the Hessian matrix [23]. Here, we found maximum ellipticity for the C–N bonds of the aromatic ring; the values are ~0.15 (MP2) and ~0.13 (DFT) respectively, which shows the anisotropic nature of bond density and these values are close to reported experimental values [21]. Whereas, in C–NO_2 bonds the predicted ellipticity values are ~0.10 (MP2) and ~0.10 (BP86), much lower than for the ring C–N bonds and reported theoretical values [22]. Overall, both methods predict almost equal ellipticity values for the same bonds and the order of ε values for the three types of bonds in the molecule are C–N > N=O > C–NO_2. Furthermore, to characterize the bond strength and to compare the predicted charge density results with the bond dissociation energy (BDE), we have calculated the BDE of various bonds of the molecule. The calculated values of BDE of ring C–N bonds and the NO_2 group attached to C–N bonds are ~91.4 and 56.2 kcal/mol, respectively. This confirms that the nitro group attached to C–N bonds are the weakest bonds in the molecule. Relatively, these BDE values are lower than for the TATB molecule (76.8 kcal/mol) [24]. Chung et al. [25] reported that a molecule having a BDE value higher than 20 kcal/mol has a barrier for the dissociation of the bond. Molecules with such types of bond can be considered as viable candidates for high energy density molecules. Hence, TNTA is a stable molecule. The BDE and Laplacian of electron density of C–NO_2 bonds give an excellent correlation, and the fact that these bond charges are highly depleted confirms that these bonds are the weakest bonds in the molecule.

Molecular stability and oxygen balance

The band gap between the highest occupied molecular orbital (HOMO) and the lowest unoccupied orbital (LUMO) has been suggested to be related to the sensitivity or stability of the explosive [26]. Fukui et al. [27] have observed for the first time the prominent role played by the highest occupied molecular orbital (HOMO) and the lowest unoccupied molecular orbital (LUMO) in governing the chemical reactions of compounds. The principle of easiest transition (PET) states that the smaller the band gap ($\Delta E_{LUMO\text{-}HOMO}$) between HOMO and LUMO, the easier will be the electron transition and the lesser the stability [28]. The DFT method predicts that the band gap ($\Delta E_{LUMO\text{-}HOMO}$) of the TNTA molecule is 12.49 eV, which is found to be much larger than for the energetic propellant molecules TNB, TNT and TATB, for which the respective values are 5.007, 4.925 and 4.054 eV. This indicates that TNTA is a very stable molecule (Table 4).

Overall, TNTA is a stable molecule, and the stability here refers to a chemical process with electron transfer or electron excitation in the molecule.

Table 3. Comparison of the energy gap, oxygen balance (OB%) and H_{50}% of TNTA with reported explosive molecules

Compound	OB %	HOMO (eV)	LUMO (eV)	$\Delta E_{LUMO-HOMO}$ (eV)	H_{50}% (m)
TNTA	+2.77	-13.551	-1.088	12.490	4.20
HNB	+3.45	-	-	-	0.10
PNA	+1.89	-	-	-	0.14
TATB	-2.33	-7.102	-3.292	4.054	4.80
TNT	-3.08	-7.891	-2.099	4.925	1.64
TNB	-1.41	-9.905	-4.898	5.007	1.49

Table 4. Electrostatic potential (e/Å) at the bond mid-points V_{mid}

Bonds	MP2		BP86	
	MPA	NPA	MPA	NPA
C(1)–N(1)	0.35	0.29	0.30	0.16
C(1)–N(2)	0.35	0.29	0.30	0.16
C(2)–N(2)	0.35	0.29	0.30	0.16
C(2)–N(3)	0.35	0.29	0.30	0.16
C(3)–N(3)	0.35	0.29	0.30	0.16
C(3)–N(1)	0.35	0.29	0.30	0.16
C(1)–N(4)	0.81	1.75	0.76	1.37
C(3)–N(6)	0.81	1.75	0.76	1.37
C(2)–N(5)	0.81	1.75	0.76	1.37
N(6)–O(5)	-0.07	0.34	-0.03	0.30
N(6)–O(6)	-0.07	0.34	-0.03	0.30
N(5)–O(3)	-0.07	0.34	-0.03	0.30
N(5)–O(2)	-0.07	0.34	-0.03	0.30
N(4)–O(1)	-0.07	0.34	-0.03	0.30
N(4)–O(2)	-0.07	0.34	-0.03	0.30

Oxygen balance (OB) is one of the important properties of energetic materials. It is defined as “the amount of oxygen, expressed in weight percent, liberated as a result of complete conversion of the explosive material to carbon dioxide, water, sulfur dioxide, aluminum oxide, etc. [29- 31]. A negative oxygen balance produces a greater quantity of CO and a positive oxygen balance produces

more NO_x gases. The equation for the oxygen balance (OB) is:

$$OB_{100} = \frac{100(2n_O - n_H - 2n_C - 2n_{COO})}{M} \quad (3)$$

where n_O and n_H represent the number of atoms of the corresponding elements in the molecule, n_{COO} is the number of carboxyl groups (for TNTA this is zero, as there are no such groups in this molecule), and M is the molecular weight. The calculated oxygen balance of the TNTA molecule is found to be positive and the value is 2.7% (Table 3). This value has been compared with other reported explosives having positive OBs (HNB ~3.45%, PNA ~ 1.89%) as well as negative OBs (TNT -3.08%; TNB -1.41%; TATB -2.33%; RDX -22%; HMX -22%). The OB of TNTA falls between that of HNB and PNA.

Furthermore, using OB and the nitro group charges (QNO_2), we have calculated the impact sensitivity of the TNTA molecule [32, 33]. These two parameters provide a new insight into the effect of molecular structure on the impact sensitivity. The impact sensitivity equation for the TNTA molecule is [32]:

$$H_{50}\% = 0.1926 + 98.64QNO_2^2 - 0.03405OB_{100}$$

A close inspection of the structural parameters of this equation provides the physical insight into the structure-impact sensitivity relationship. The predicted H_{50}% value for the TNTA molecule (4.2 m) is slightly lower than the reported value for the TATB molecule (Table 3) (4.8 m).

Relation between the molecular electrostatic potential and impact sensitivity

The molecular electrostatic potential (MEP) [34, 35] explores the polarization and charge transfer effects within the molecule. This parameter can be used to predict the electrophilic and nucleophilic sites in the molecule where chemical reactions are expected to occur. Due to the charge complementarity, it gives novel insights into the impact sensitivity of explosives. Figure 5 shows the theoretical MEP obtained from the MP2 level of calculation, with the electronegative and electropositive regions of the molecule. A large electronegative potential is found in the vicinity of the $–NO_2$ groups, and a small electronegative region near the ring N–atoms.

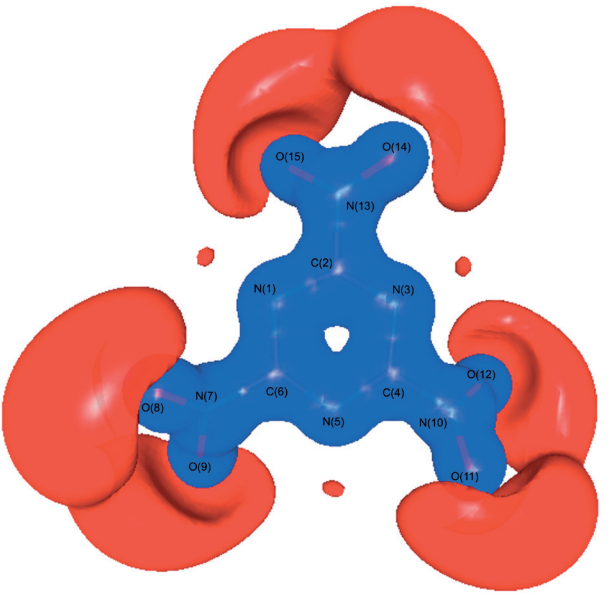

Figure 5. Isosurface representation of electrostatic potential of the TNTA molecule. Blue: positive potential (+0.5 e Å^{-1}), red: negative potential (-0.3 e Å^{-1}).

According to the Politzer [31], Owens [36] and Rice et al. [4] hypothesis, the ESPs of nitro-aromatic systems, the molecular electrostatic potential has a parallel relationship with the impact sensitivity of the molecule. Here, we also explore the parallel relationship by calculating the potential build-up at the midpoint of all bonds of the TNTA molecule, according to the equation:

$$V_{mid} = \frac{q_i}{0.5r} + \frac{q_j}{0.5r} \tag{4}$$

where q_i and q_j are the atomic charges for i^{th} and j^{th} atoms and r is the bond distance. Here, the V_{mid} calculations (Table 4) were performed for the MPA and NPA charges obtained from both the MP2 and BP86 methods at the 6-311G* basis set. This study reveals that for the nitro group attached to C–N bonds, the V_{mid} values are high compared with other bonds in the molecule. The calculated V_{mid} values from C–N bonds, which are the sensitive bonds in the molecule, for both MPA and NPA charges of the MP2 and DFT methods are ~0.81 (MPA)/~1.75 (NPA) and ~0.76 (MPA)/~1.37 e/Å (NPA) respectively. Figure 6

shows the relationship between the bond charge depletion $\nabla^2\rho_{bcp}(r)$ and the impact sensitivity (V_{mid}) of each bond in the molecule. The map explicitly shows that highly charge-depleted bonds (C–NO_2) are the sensitive bonds in the molecule.

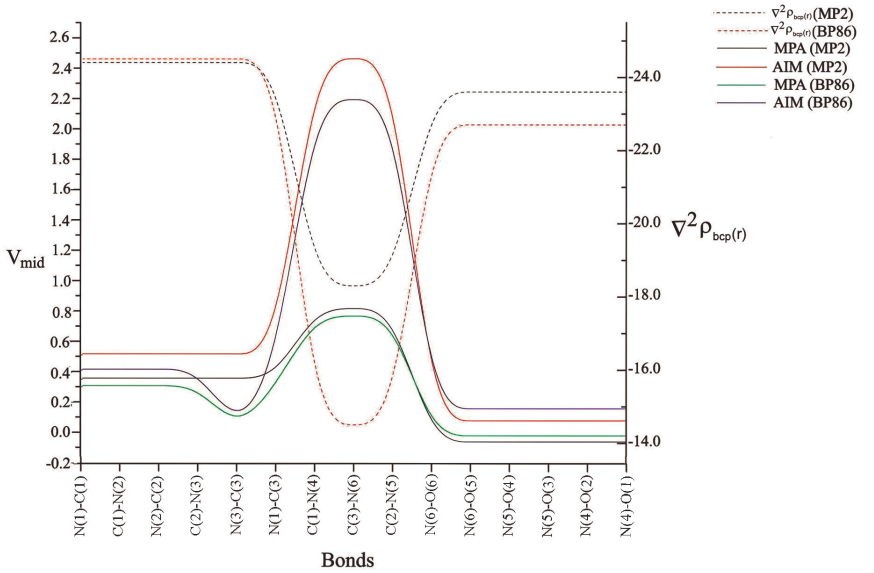

Figure 6. Relationship between $\nabla^2\rho_{bcp}(r)$ and ESP at the bond midpoints V_{mid}.

Conclusion

The bond topological and electrostatic properties of the energetic TNTA molecule were carefully evaluated by *ab initio* (MP2) and density functional theory (BP86) calculations. For both levels of calculation, the C–NO_2 bonds have low charge accumulation at the bond critical point, which indicates that the charges of the bonds are highly depleted compared with all other bonds in the molecule. The charge accumulation in C_{ar}–N_{ar} and N=O bonds is found to be high compared with the NO_2 group attached to C–N bonds; their corresponding high negative $\nabla^2\rho_{bcp}(r)$ confirms its high solidarity. The charges in the C–NO_2 bonds are highly depleted and this charge depletion has been further confirmed from the energy density calculations. Compared with other reported explosives, the TNTA molecule exhibits a wide band gap (12.49 eV) and a positive oxygen balance (2.77%). Using the oxygen balance and the nitro group charges, we

have calculated the impact sensitivity (H_{50}%) of the TNTA molecule as 4.2 m. Furthermore, the sensitivity calculation based on ESP (V_{mid}) predicts that the nitro groups attached to C–N bonds are more sensitive than the other bonds in the molecule. On the basis of these findings, we conclude that the NO_2 group attached to C–N bonds are very weak bonds in the molecule. These bonds may rupture first and initiate the detonation process when the material is exposed to external stimuli. Importantly, the present study also confirms the fair relation between the charge depletion and the bond sensitivity of the molecule.

References

[1] (a) Butcher R.J., Bottaro J.C., Gilardi R., Ammonium 1,3,4,6-tetranitro-2,5-diazapentalene, *Acta Cryst*., **2003**, *E59*, o1149-o1150; (b) Butcher R. J., Bottaro J.C., Gilardi R., 1-Nitro-7,8-diazapentalene, *Acta Cryst*., **2003**, *E59*, o1777-o1779.

[2] (a) Butcher R.J., Bottaro J.C., Gilardi R., Potassium 1,3,4,6-tetranitro-2,5-diazapentalene, *Acta Cryst*., **2003**, *E59*, m591-m593; (b) Butcher R.J., Bottaro J.C., Gilardi R., 1,3,4-Trinitro-7,8-diazapentalene, *Acta Cryst*., **2003**, *E59*, o1780-o1782.

[3] Muray J.S., Lane P., Politzer P., Relationships Between Impact Sensitivities and Molecular Surface Electrostatic Potentials of Nitroaromatic and Nitroheterocyclic Molecules, *Mol. Phys,* **1995**, *85*(1), 1-8.

[4] Rice B.M., Hare J.J., A Quantum Mechanical Investigation of the Relation between Impact Sensitivity and the Charge Distribution in Energetic Molecules, *J. Phys. Chem. A*., **2002**, *106*, 1770-1783.

[5] Agrawal J.P., *High Energy Materials*, Wiley-VCH, Weinheim, **2011**.

[6] Klapötke T.M., *Chemistry of High–Energy Materials*, Wdeg, Berlin, **2011**.

[7] (a) David Stephen A., Kumaradhas P., Pawar R.B., Charge Density Distribution, Electrostatic Properties, and Impact Sensitivity of the High Energetic Molecule TNB: A Theoretical Charge Density Study, *Propellants, Explos., Pyrotech*., **2011**, *36*, 168-174; (b) David Stephen A., Revathi M., Asthana S. N., Pawar R.B., Kumaradhas P., Probing the Weakest Bond and the Cleavage of p-Chlorobenzaldehyde Diperoxide Energetic Molecule via Quantum Chemical Calculations and Theoretical Charge Density Analysis, *Int. J. Quant. Chem*., **2010**, *111*(14), 3741-3754.

[8] David Stephen A., Pawar R.B., Kumaradhas P., Exploring the Bond Topological Properties and the Charge Depletion-impact Sensitivity Relationship of High Energetic TNT Molecule via Theoretical Charge Density Analysis, *J.Mol. Struct. (THEOCHEM)*., **2010**, *959*, 55-63.

[9] Srinivasan P., Asthana S.N., Pawar R.B., Kumaradhas P., A Theoretical Charge Density Study on Nitrogen-rich 4,4',5,5'-Tetranitro-2,20-bi-1H-imidazole (TNBI) Energetic Molecule, *Struct. Chem.*, **2011**, *22*, 1213-1220.

[10] Korkin A.A., Bartlett R.J., Theoretical Prediction of 2,4,6-Trinitro-1,3,5-triazine (TNTA). A New, Powerful, High-Energy Density Material?, *J. Am. Chem. Soc*.,

1996, *118*, 12244-12245.

[11] Li J., An Ab Initio Theoretical Study of 2,4,6-Trinitro-1,3,5-Triazine, 3,6-Dinitro-1,2,4,5-Tetrazine, and 2,5,8-Trinitro-Tri-s-Triazine, *Propellants, Explos. Pyrotech*., **2008**, *33*, 443-447.

[12] Kohn W., Sham L.J., Self-Consistent Equations Including Exchange and Correlation Effects, *Phys. Rev*., **1965**, *140*, A1133-A1138.

[13] Gillespie R.J., Popelier P.L.A., *Chemical Bonding and Molecular Geometry*, Oxford University Press, **2001**.

[14] Frisch M.J., Trucks G.W., Schlegel H.B., Scuseria G.E., Robb M.A., Cheeseman J.R., Montgomery J.A., Vreven Jr., Kudin K.N., Burant J.C., Millam J.M., Iyengar S.S., Tomasi J., Barone V., Mennucci B., Cossi M., Scalmani G., Rega N., Petersson G.A., Nakatsuji H., Hada M., Ehara M.P., Toyota K., Fukuda R., Hasegawa J., Ishida M., Nakajima T., Honda Y., Kitao O., Nakai H., Klene M., Li X., Knox J.E., Hratchian H.P., Cross J.B., Adamo, Jaramillo J., Gomperts R., Stratmann R.E., Yazyev O., Austin A.J., Cammi R., Pomelli C., Ochterski J.W., Ayala P.Y., Morokuma., Voth G.A., Salvador P., Dannenberg J.J., Zakrzewski V.G., Dapprich S., Daniels A.D., Strain M.C., Farkas O., Malick D.K., Rabuck A.D., Raghavachari K., Foresman J.B., Ortiz J.V., Cui Q., Baboul A.G., Clifford S., Cioslowski J., Stefanov B.B., Liu G., Liashenko A., Piskorz P., Komaromi I., Martin R.L., Fox D.J., Keith T., Al-Laham M.A., Peng C.Y., Nanayakkara A., Challacombe M., Gill P.M.W., Johnson B., Chen W., Wong M.W., Gonzalez C., Pople J.A., *Gaussian 03, Revision D.1*, Gaussian, Inc., Wallingford, CT, **2005**.

[15] Cheeseman J., Keith T.A., Bader R.F.W., *AIMPAC Program Package*, McMaster University Hamilton, Ontario, **1992**.

[16] Wiberg K.B., Application of the Pople-santry-segal CNDO Method to the Cyclopropylcarbinyl and Cyclobutyl Cation and to Bicyclobutane, *Tetrahedron*, **1968**, *24*(3), 1083-1096.

[17] Koritsanszky T., Macchi P., Gatti C., Farrugia L.J., Mallinson P.R., Volkov A., Richter T., *XD-2006. A Computer Program Package for Multipole Refinement and Topological Analysis of Charge Densities and Evaluation of Intermolecular Energies from Experimental or Theoretical Structure Factors*, Version 5.33, **2007**.

[18] Gillespie R.J., Popelier P.L.A., *Chemical bonding and molecular geometry*, Oxford University Press, New York, **2001**.

[19] Coppens P., *X-ray charge densities and chemical bonding*, Oxford University Press, New York., **1997**.

[20] Stash A., Tsirelson V., WinXPRO: a Program for Calculating Crystal and Molecular Properties Using Multipole Parameters of the Electron Density, *J. Appl. Cryst*., **2002**, *35*, 371-373.

[21] Muzet N., Artacho E., Lecomte C, Jelsch C., Guillot B., Muzet N., Artacho E., Experimental and Theoretical Electron Density Studies in Large Molecules: NAD^+, β-Nicotinamide Adenine Dinucleotide, Benoît Guillot, *J. Phys. Chem*., **2003**, *B107*, 9109-9121.

[22] David Stephen A., Srinivasan P., Kumaradhas P., Bond Charge Depletion,

Bond Strength and the Impact Sensitivity of High Energetic 1,3,5-Triamino-2,4,6-trinitrobenzene (TATB) Molecule: A Theoretical Charge Density Analysis, *Comput. Theo. Chem*., **2011**, *967*, 250-256.

[23] (a) Bader R.F.W., *Atoms in Molecule: A Quantum Theory*; Clarendon press: Oxford, UK, **1990**; (b) Popelier P.L.A., *Atom in Molecules an Introduction*, Pearson Edition: Harlow, UK, **1999**.

[24] Owens F.J., Calculation of Energy Barriers for Bond Rupture in Some Energetic Molecules, *J. Mol. Struct. (THEOCHEM),* **1996**, *370*(1), 11-16.

[25] Chung G., Schmidt M.W., Gordon M.S., An Ab Initio Study of Potential Energy Surfaces for N_8 Isomers, *J. Phys. Chem*., **2000**, *A104*, 5647-5650.

[26] Ghule V.D., Sarangapani R., Jadhav P.M., Pandey R.K., Computational Design and Structure–property Relationship Studies on Heptazines, *J. Mol. Model.*, **2011**, *17,* 2927-2937.

[27] Fukui K., Yonezawa T., Shingu H., A Molecular Orbirtal Theory of Reactivity in Aromatic Hydrocarbons, *J. Chem. Phys*., **1952**, *20*, 722-725.

[28] Gobel M., Karaghiosoff K., Klapotke T.M., Piercey D.G., Stierstorfer J., Nitrotetrazolate-2*N*-oxides and the Strategy of *N*-Oxide Introduction, *J. Am. Chem. Soc.*, **2010**, *132*(48),17216-17226.

[29] Thottempudi V., Gao H., Shreeve J.M., Trinitromethyl-Substituted 5-Nitro- or 3-Azo-1,2,4-triazoles: Synthesis, Characterization, and Energetic Properties, *J. Am. Chem. Soc*., **2011**, *133*(16), 6464-6471.

[30] Liu Y., Gong X., Wang L., Wang G., Xiao H., Substituent Effects on the Properties Related to Detonation Performance and Sensitivity for 2,2′,4,4′,6,6′-Hexanitroazobenzene Derivatives, *J. Phys. Chem. A*., **2011**, *115*(9), 1754-1762.

[31] Politzer P., Laurence P.R., Abrahmsen L., Zilles B.A., SjobergP., The Aromatic C–NO_2 Bond as a Site for Nucleophilic Attack, *Chemical Physics Letters*., **1984**, *111*(1), 75-78.

[32] Cao C., Gao S., Two Dominant Factors Influencing the Impact Sensitivities of Nitrobenzenes and Saturated Nitro Compounds, *J. Phys. Chem B*, **2007**, *111*, 12399.

[33] Keshavarz M. H., Pouretedal H. R., Simple Empirical Method for Prediction of Impact Sensitivity of Selected Class of Explosives, *J. Hazard. Mater*., **2005**, *A124*, 27.

[34] Draskovic B.M., Bogdanovic G.A., Neelakandan M.A., Chamayou A.C., Thalamuthu S., Avadhut Y.S., Banerjee S., Janiak D., N-o-Vanillylidene-L-histidine: Experimental Charge Density Analysis of a Double Zwitterionic Amino Acid Schiff-Base Compound., *Cryst. Grow. Design,* **2010**, *10*, 1665.

[35] Brinck T., Jin P., Ma Y., Murray J.S., Politzer P., Segmental Analysis of Molecular Surface Electrostatic Potentials: Application to Enzyme Inhibition, *J. Mol. Model*., **2003**, *9*, 77-83.

[36] Owens F.J., Jayasuriya K., Abrahmsen L., Politzer P., Computational Analysis of Some Properties Associated with the Nitro Groups in Polynitroaromatic Molecules, *Chem. Phys. Lett*., **1985**, *116*(5), 434-438.